Title

Dual Action Calcium-Sensing Receptor Modulator Unmasks Novel Mode-Switching Mechanism

Journal

ACS Pharmacology & Translational Science, 1(2)

ISSN

2575-9108

Authors

Gregory, Karen J
Kufareva, Irina
Keller, Andrew N
et al.

Publication Date

2018-11-09

DOI

10.1021/acsptsci.8b00021

Peer reviewed

ACS Pharmacology & Translational Science

Article

Cite This: ACS Pharmacol. Transl. Sci. 2018, 1, 96−109

pubs.acs.org/ptsci

Dual Action Calcium-Sensing Receptor Modulator Unmasks Novel Mode-Switching Mechanism

Karen J. Gregory,[†] Irina Kufareva,[‡] Andrew N. Keller,[†] Elham Khajehali,[†] Hee-Chang Mun,[§] Mahvash A. Goolam,[§] Rebecca S. Mason,[∥] Ben Capuano,[†] Arthur D. Conigrave,[§] Arthur Christopoulos,[†] and Katie Leach*[,†]

[†]Drug Discovery Biology and Department of Pharmacology, Monash Institute of Pharmaceutical Sciences, 381 Royal Parade, Monash University, Parkville, Victoria 3052, Australia

[‡]Skaggs School of Pharmacy & Pharmaceutical Sciences, University of California, 9500 Gilman Drive, La Jolla, San Diego, California MC 0747, United States

[§]School of Life and Environmental Sciences, Charles Perkins Centre, and [∥]Physiology and Bosch Institute, Building F13, University of Sydney, Sidney, New South Wales 2006, Australia

Supporting Information

ABSTRACT: Negative allosteric modulators (NAMs) of the human calcium-sensing receptor (CaSR) have previously failed to show efficacy in human osteoporosis clinical trials, but there is now significant interest in repurposing these drugs for hypocalcemic disorders and inflammatory lung diseases. However, little is known about how CaSR NAMs inhibit the response to endogenous activators. An improved understanding of CaSR negative allosteric modulation may afford the opportunity to develop therapeutically superior CaSR-targeting drugs. In an attempt to elucidate the mechanistic and structural basis of allosteric modulation mediated by the previously reported NAM, calhex231, we herein demonstrate that calhex231 actually potentiates or inhibits the activity of multiple CaSR agonists depending on whether it occupies one or both protomers in a CaSR dimer. These findings reveal a novel mechanism of mode-switching at a Class C G protein-coupled receptor that has implications for drug discovery and potential clinical utility.

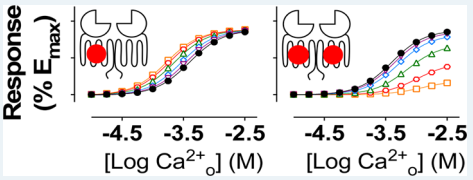

KEYWORDS: *calcium-sensing receptor, calhex231, allosteric modulator*

The human calcium-sensing receptor (CaSR) is a Class C G protein-coupled receptor (GPCR). It is abundantly expressed in the parathyroid glands where it regulates extracellular calcium (Ca^{2+}_o) homeostasis via inhibitory control of parathyroid hormone (PTH) secretion in response to elevations in serum Ca^{2+}_o levels.[1,2] Accordingly, the positive allosteric modulators (PAMs), cinacalcet and etelcalcitide, are currently FDA approved for the treatment of hyperparathyroidism, although their use remains limited due to adverse side effects. CaSR negative allosteric modulators (NAMs) have undergone clinical testing for osteoporosis, but have so far failed to promote sufficiently significant increases in bone mass and density, potentially because they do not stimulate adequate PTH release, do not demonstrate the desired pharmacokinetic profile, and/or have off-target effects in bone cells.[3] These limitations attest to the ongoing need for a better understanding of CaSR allostery, which, in contrast to allosteric mechanisms at other Class C GPCRs such as the metabotropic glutamate (mGlu) receptors, has not been explored in detail.

Recently, we combined pharmacological and analytical methods with a detailed structure−function analysis to probe the structural basis of CaSR allostery. We found that the CaSR possesses a hitherto unappreciated extended 7 transmembrane (7TM) domain cavity that accommodates binding sites for small molecule PAMs and NAMs.[4,5] Importantly, we revealed that the arylalkylamines, cinacalcet (PAM), NPSR568 (PAM), and NPS2143 (NAM), occupy a common binding pocket and contact many of the same amino acid residues within this pocket.[4,5] Nonetheless, subtle differences in ligand−receptor interactions drive negative versus positive modulation of CaSR signaling by NPS2143 or cinacalcet and NPSR568, respectively.[4−8] In contrast to the arylalkylamines, the structurally and pharmacologically distinct PAM, AC265347, bound to a partly overlapping but discrete site at the bottom of the extended cavity.[4]

Molecular modeling and mutagenesis studies are consistent with the hypothesis that other reported arylalkylamine modulators share the cinacalcet/NPSR568 and NPS2143 binding site.[6−8] However, the ligand−receptor interactions that govern positive versus negative modulation are not universally shared among all arylalkylamines. For instance, Ala substitution of $Arg680^{3.32}$ (numbering shown in superscript is based on that assigned in Dore et al.[9]) in TM3 attenuates NPS2143 binding but has no effect on cinacalcet,[4] whereas

Received: July 13, 2018
Published: September 12, 2018

DOI: 10.1021/acsptsci.8b00021
ACS Pharmacol. Transl. Sci. 2018, 1, 96−109

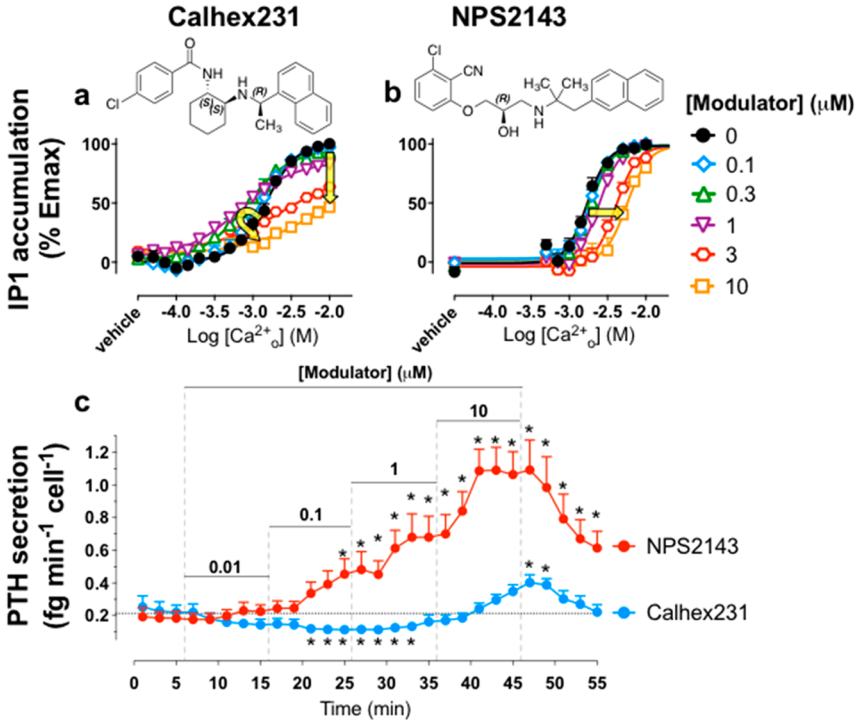

Figure 1. Calhex231 is a mixed positive and negative modulator of the CaSR. (a,b) Ca^{2+}_o-mediated IP1 accumulation in the absence or presence of calhex231 (a) or NPS2143 (b) was determined in CaSR-HEK293 cells in 0.1 mM ambient Ca^{2+}_o, for which the modulator and Ca^{2+}_o were co-incubated for 45 min. Data are mean + s.e.m. from 3 to 4 experiments performed in duplicate. Curves are the best fit to eq 1, and parameters describing the curves are shown in Supplemental Table 1. Direction and magnitude of arrows demonstrate the influence of calhex231 on agonist pEC_{50} or E_{max}, with mixed mode activity denoted by a U-turn arrow. (c) Calhex231 modulation of PTH secretion from primary human parathyroid cells was determined in 1.2 mM ambient Ca^{2+}_o using an Immulite 2000 analyzer. Data are mean + s.e.m. from 5 experiments performed as single determinations. *Significantly different to in the absence of NAM, $p < 0.05$, two-way repeated measures ANOVA with Dunnett's multiple comparisons post-test.

cinacalcet but not NPS2143 binding is altered by Ala substitution of Phe821$^{6.53}$ or Trp818$^{6.50}$ in TM6.[4,7,8] Interestingly, like cinacalcet, Phe821$^{6.53}$Ala or Trp818$^{6.50}$Ala but not Arg680$^{3.32}$Ala also altered the activity of another arylalkylamine modulator, calhex231,[7,8] which was derived from a PAM scaffold, but to date has been widely and consistently classified as a NAM based on its ability to inhibit a single concentration of the CaSR's orthosteric agonist, Ca^{2+}_o.[7,8,10] However, we have recently highlighted that at the mGlu receptors, assessing modulator activity against a single agonist concentration in a single assay can lead to substantial misinterpretation of modulator pharmacology.[11−13] Therefore, in an attempt to perform the first in-depth pharmacological characterization of calhex231, we sought to evaluate its ability to modulate CaSR responsiveness to a range of Ca^{2+}_o concentrations using two different measures of receptor activity. In doing so, we reveal that calhex231 displays mixed modes of PAM and NAM activity in a concentration-dependent, and physiologically relevant, manner. This finding can be reconciled mechanistically by calhex231 interacting cooperatively with itself across the CaSR dimer. Our findings have important implications for the screening, design, and utility of CaSR PAMs and NAMs as chemical probes or therapeutics, and have potential applicability to "mode-switching" at other dimeric GPCRs.

RESULTS

Calhex231 Is a Mixed PAM and NAM. Calhex231 was originally reported as a CaSR NAM based on its ability to inhibit a single maximum activating concentration of Ca^{2+}_o in an IP accumulation assay, at the rat CaSR expressed in CHO cells.[10] We first sought to confirm and extend these findings by evaluating the effect of calhex231 on a range of Ca^{2+}_o concentrations in an IP1 accumulation assay in HEK293 cells stably expressing the human CaSR (CaSR-HEK293). Notably, the buffer for these assays contained low (0.1 mM) ambient Ca^{2+}_o for consistency with previous studies.[10,14] In agreement with previously published data,[7,8,10] 3−10 μM calhex231 exhibited NAM activity, inhibiting IP1 accumulation stimulated by Ca^{2+}_o in CaSR-HEK293 cells (Figure 1a) by decreasing the potency (pEC_{50}) and maximal response (E_{max}) of the Ca^{2+}_o concentration−response curve (Supplemental Table 1). Surprisingly, however, 0.1−1 μM calhex231 behaved as a PAM, enhancing Ca^{2+}_o potency and resulting in a leftward shift in the Ca^{2+}_o concentration−response curve (Figure 1a and Supplemental Table 1). Under these same conditions, the prototypical NAM, NPS2143, only reduced Ca^{2+}_o potency in a concentration-dependent manner (Figure 1b and Supplemental Table 1), as expected.

Of note, all CaSR PAMs that we have tested previously under the same assay conditions had no effect on Ca^{2+}_o E_{max} in IP1 assays,[15] therefore the calhex231-mediated reduction in potency and E_{max} is unlikely to be due to PAM-mediated receptor desensitization. As confirmation, CaSR-HEK293 cells were treated with 1 μM of the broad-spectrum protein kinase C (PKC) inhibitor, Go6983, for 30 min prior to ligand addition, because PKC has previously been implicated in CaSR desensitization.[16] Go6983 had no effect on calhex231-

DOI: 10.1021/acsptsci.8b00021
ACS Pharmacol. Transl. Sci. 2018, 1, 96−109

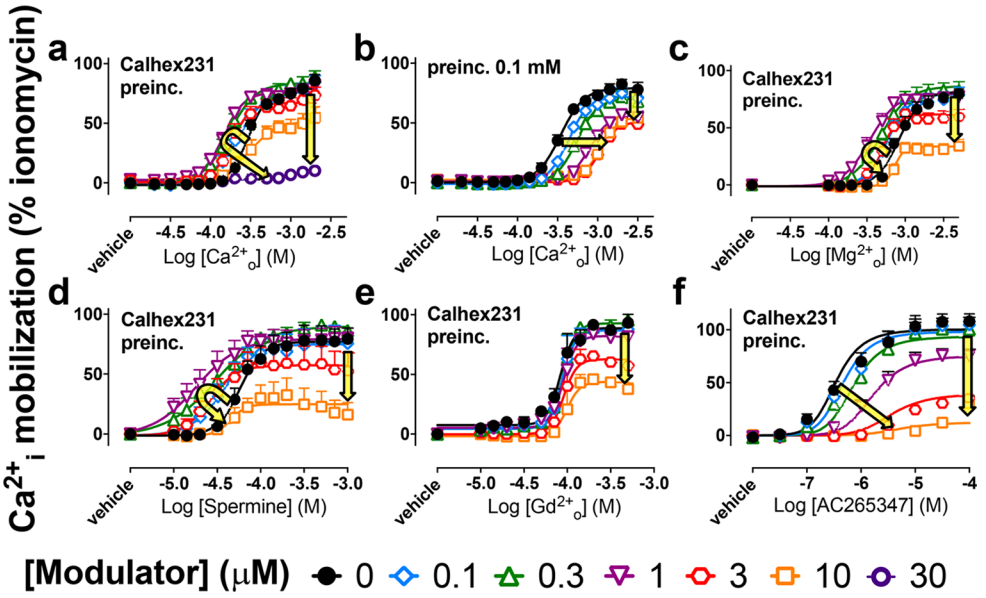

Figure 2. Calhex231 modulation at the CaSR is probe- and context-dependent. Agonist-mediated Ca^{2+}_i mobilization in the absence or presence of calhex231 or NPS2143 was determined in CaSR-HEK293 cells in 0.1 mM ambient Ca^{2+}_o. Data are mean + s.e.m. from 3 to 6 experiments performed in duplicate. (a,b) Peak Ca^{2+}_o-mediated Ca^{2+}_i mobilization (within 60 s) following preincubation with calhex231 (a) or NPS2143 (b) for 20 min prior to Ca^{2+}_o addition. (c–f) Peak agonist-mediated Ca^{2+}_i mobilization following preincubation with modulator for 20 min prior to Mg^{2+}_o (c), spermine (d), Gd^{3+}_o (e), or AC265347 (f) addition. Curves are the best fit to eq 1 (a–e), or eq 3 (f). Direction and magnitude of arrows demonstrate the influence of calhex231 on agonist pEC_{50} or E_{max}, with mixed mode activity denoted by a U-turn arrow.

mediated PAM or NAM activity (Supplemental Figure 1a). Further, previous studies indicated that CaSR cell surface expression is not reduced upon agonist or PAM exposure,[17] and accordingly, calhex231 and cinacalcet had no effect on CaSR cell surface expression in our CaSR-HEK293 cells (Supplemental Figure 1b). Finally, the E_{max} reduction in response to calhex231 was not due to cytotoxicity, since 45 min of calhex231 incubation (10 μM) with or without 2 mM Ca^{2+}_o did not alter propidium iodide uptake into CaSR-HEK293 cells in comparison to vehicle control (data not shown). Therefore, low calhex231 concentrations mediate on-target PAM activity, whereas higher concentrations mediate NAM activity in IP1 accumulation assays. Such observations cannot be explained by a monotonic mechanism in which the modulator only increases or only decreases the agonist response.

Calhex231 Both Inhibits and Stimulates PTH Release from Primary Human Parathyroid Cells. To determine whether the dual PAM and NAM activity of calhex231 in CaSR-HEK293 cells was physiologically relevant, we examined calhex231-mediated modulation of PTH secretion from human parathyroid cells that endogenously express the CaSR. These experiments were performed in the presence of 1.2 mM ambient Ca^{2+}_o to reflect physiological serum Ca^{2+}_o concentrations. As expected for a CaSR NAM, NPS2143 (0.1–10 μM) robustly stimulated PTH release (Figure 1c). In contrast, 0.1–1 μM calhex231 weakly but significantly reduced (2-fold) PTH secretion (commensurate with CaSR PAM activity), whereas PTH secretion was significantly increased in response to 10 μM calhex231 (Figure 1c). These results indicate that calhex231, acting at endogenously expressed CaSRs, exerts both PAM and NAM activity on one of the receptor's key physiological functions.

Calhex231-Mediated Allostery Is Both Probe and Context-Dependent. We have found that CaSR preincubation with NPS2143 prior to agonist addition unmasks NAM activity in a Ca^{2+}_i mobilization assay.[14] Therefore, to determine whether calhex231 also demonstrated mixed modulatory activity in this assay, we employed a Ca^{2+}_i mobilization "preincubation paradigm".[4,14] Similar to IP1 accumulation assays, in 0.1 mM ambient Ca^{2+}_o, calhex231 was both a PAM and a NAM of Ca^{2+}_o-mediated Ca^{2+}_i mobilization depending on its concentration (Figure 2a and Supplemental Table 2), whereas NPS2143 was a pure NAM under these conditions (Figure 2b and Supplemental Table 2). Interestingly, although NPS2143 only partially inhibited CaSR signaling, as evidenced by a saturable reduction in Ca^{2+}_o potency and E_{max} (i.e., the maximum inhibitory NPS2143 effect occurred at 3 μM, with no greater inhibition of Ca^{2+}_o by 10 μM NPS2143) (Figure 2b), 30 μM calhex231 completely abrogated CaSR signaling (Figure 2a).

Previously, we showed that PAM preincubation results in CaSR-mediated desensitization of Ca^{2+}_i mobilization, reducing agonist E_{max}.[14] Accordingly, in the present study, a 20 min preincubation with the PAM, cinacalcet, reduced the Ca^{2+}_o E_{max} (Supplemental Figure 1c), and also reduced Ca^{2+}_i mobilization stimulated by trypsin acting at endogenously expressed protease activated receptor 2 (PAR2) in CaSR-HEK293 cells (Supplemental Figure 1d), indicating depletion of Ca^{2+}_i stores. In contrast, calhex231 had no effect on trypsin-mediated Ca^{2+}_i mobilization (Supplemental Figure 1e), indicating that, unlike cinacalcet, calhex231 did not suppress E_{max} via depletion of Ca^{2+}_i stores.

We have previously shown that allosteric modulators can differentially modulate different CaSR agonists via "probe-dependence".[18] Therefore, we next assessed calhex231 modulation of other orthosteric and allosteric CaSR agonists (probes). Calhex231 had positive and negative cooperativity with the endogenous CaSR agonists, Mg^{2+}_o and spermine (Figure 2c,d), whereas it was a pure NAM of the exogenous

DOI: 10.1021/acsptsci.8b00021
ACS Pharmacol. Transl. Sci. 2018, 1, 96–109

trivalent cation, gadolinium (Gd^{3+}_o), and the small molecule PAM-agonist, AC265347 (Figure 2e,f), indicating that calhex231 allostery is probe-dependent.

To better show the PAM activity mediated by calhex231, we next used an agonist and modulator "co-addition" paradigm (the modulator is added simultaneously with the agonist) in the Ca^{2+}_i mobilization assay.[4,15] 0.1−10 μM calhex231 caused only a leftward shift in the Ca^{2+}_o concentration−response curve (Figure 3a), with Ca^{2+}_o potency significantly increased in

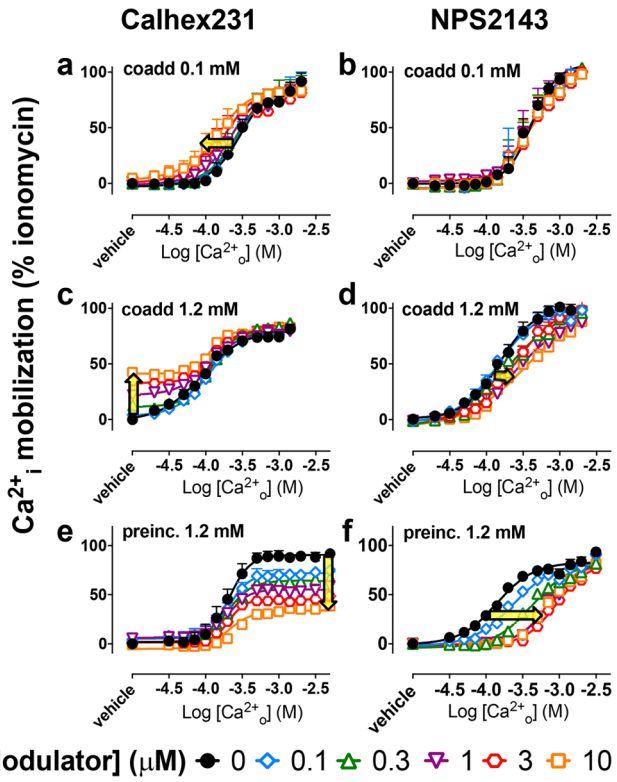

Figure 3. Allosteric modulation at the CaSR is context-dependent. Peak Ca^{2+}_o-mediated Ca^{2+}_i mobilization (within 60 s) in the absence or presence of calhex231 or NPS2143 was determined in CaSR-HEK293 cells. Data are mean + s.e.m. from 3 experiments performed in duplicate. (a,b) Ca^{2+}_i mobilization following coaddition of calhex231 (a) or NPS2143 (b) and Ca^{2+}_o in the presence of 0.1 mM ambient Ca^{2+}_o. (c,d) Ca^{2+}_i mobilization following coaddition of calhex231 (c) or NPS2143 (d) and Ca^{2+}_o in the presence of 1.2 mM ambient Ca^{2+}_o. (e,f) Ca^{2+}_i mobilization following "pre-incubation" of calhex231 (e) or NPS2143 (f) prior to Ca^{2+}_o addition in the presence of 1.2 mM ambient Ca^{2+}_o. Curves shown in a−f are the best fit to eq 1.

the presence of 3 and 10 μM calhex231 (Supplemental Table 3). No reduction in E_{max} was observed. Thus, calhex231 was a pure PAM under these conditions. In contrast to calhex231, and as reported previously,[14] NPS2143 displayed little activity when coadded with Ca^{2+}_o (Figure 3b and Supplemental Table 3).

When we repeated the coaddition experiments in the presence of physiological (1.2 mM) ambient Ca^{2+}_o, calhex231 again did not demonstrate any NAM activity and instead enhanced basal Ca^{2+}_i mobilization levels (Figure 3c and Supplemental Table 4), whereas NPS2143 weakly inhibited Ca^{2+}_o potency (2-fold) (Figure 3d and Supplemental Table 4). In contrast, preincubation interaction studies performed in the presence of physiological 1.2 mM ambient Ca^{2+}_o, revealed calhex231 as a pure NAM, significantly reducing Ca^{2+}_o potency and/or E_{max} in a concentration-dependent manner (Figure 3e, Supplemental Table 4). Under the same conditions, NPS2143 reduced Ca^{2+}_o potency but had no significant effect on E_{max} (Figure 3f, Supplemental Table 4). Collectively, these data demonstrate probe- and context-dependent CaSR modulation by calhex231 and support a novel mode of pharmacology for calhex231 as an allosteric modulator of Ca^{2+}_o activity, in which receptor occupancy by both the orthosteric agonist and calhex231 dictate positive versus negative cooperativity.

Calhex231 Mediates both PAM and NAM Activity via Interactions within the 7TM Domain. The Class C 7TM allosteric binding sites are considerably distant from the orthosteric binding site(s) in the N-terminal "venus flytrap" (VFT) domain. Thus, calhex231 PAM and NAM activity cannot arise from a calhex231 binding site that spans both the orthosteric and allosteric binding sites (a bitopic mode of binding). Thus, the most parsimonious explanation for the ability of calhex231 to act as both a PAM and a NAM is that it binds to two distinct allosteric sites depending on its concentration and affinity for each site. To test this hypothesis, we sought to probe the structural requirements of calhex231-mediated allostery. We first sought to determine whether calhex231 bound to both the N-terminal VFT and the 7TM domain by examining the effect of calhex231 preincubation with an N-terminally truncated CaSR stably expressed in HEK293 cells in 0.1 mM ambient Ca^{2+}_o.

At the N-terminally truncated CaSR, the Ca^{2+}_o concentration−response curve was biphasic in the absence and presence of 0−3 μM calhex231 (Figure 4a). Much like the high and low affinity Ca^{2+}_o binding sites in the VFT domain,[19] the observed high and low potency responses at the N-terminally truncated receptor may be due to Ca^{2+}_o binding to one or more high and low affinity binding sites within the 7TM domain. In all instances, the maximum Ca^{2+}_o response at the "high affinity binding site" plateaued at approximately 2 mM. We could not define the complete Ca^{2+}_o concentration−response relationship at the "lower affinity site" because Ca^{2+}_o concentrations greater than 14 mM increase intracellular Ca^{2+}_i concentrations in untransfected HEK293 cells (data not shown). Therefore, we compared the effect of calhex231 on the response stimulated by 2 mM Ca^{2+}_o and 14 mM Ca^{2+}_o. Calhex231 at 0.3−3 μM significantly enhanced the response stimulated by 2 or 14 mM Ca^{2+}_o in comparison to the control, whereas there was no significant difference in the response to Ca^{2+}_o in the presence of 10 μM calhex231 versus the control (i.e., calhex231 suppressed its own potentiation of Ca^{2+}_o-mediated signaling, but did not reduce Ca^{2+}_o E_{max} or potency in comparison to vehicle control) (Figure 4a, Supplemental Table 5), indicating that calhex231 interacts with the 7TM domain to mediate both effects.

Identification of Amino Acid Residues Essential for Calhex231 PAM and NAM Activities. We next investigated the effects of amino acid substitutions in the extended 7TM modulator binding cavity on the functional activity of calhex231. For these studies, calhex231 was preincubated with cells prior to agonist addition, and experiments were performed in the presence of 0.1 mM ambient Ca^{2+}_o for direct comparisons with our previous structure−function study.[4] Mutated residues were selected based on their contributions to the arylalkylamine binding site utilized by NPS2143 and cinacalcet.[4]

DOI: 10.1021/acsptsci.8b00021
ACS Pharmacol. Transl. Sci. 2018, 1, 96−109

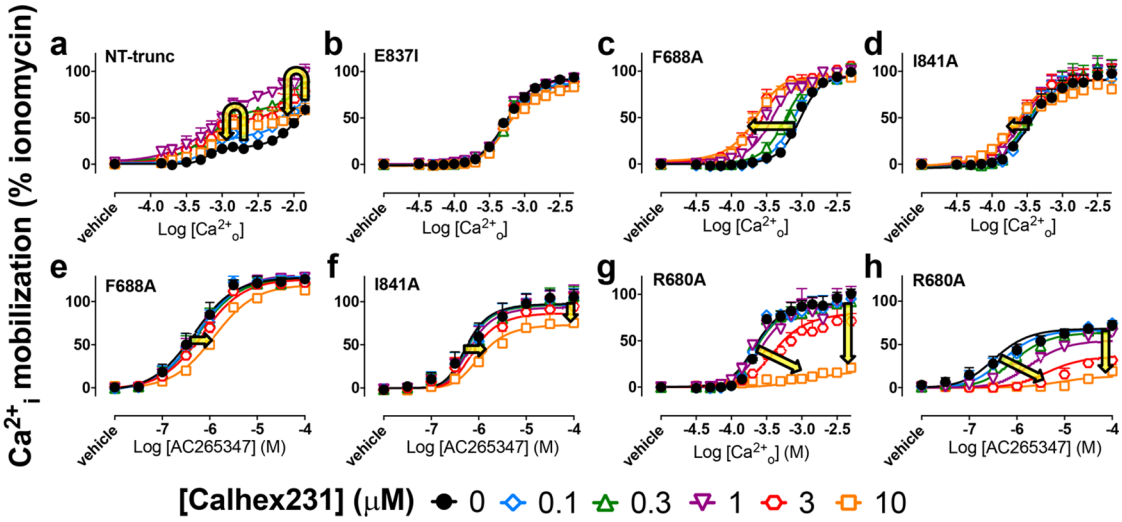

Figure 4. Calhex231 PAM and NAM activity are differentially altered by 7TM domain mutations. Ca^{2+}_o-mediated Ca^{2+}_i mobilization in the absence or presence of calhex231 was determined in mutant CaSR-expressing HEK293 cells in 0.1 mM ambient Ca^{2+}_o, following a 20 min calhex231 preincubation prior to determination of peak agonist-mediated Ca^{2+}_i mobilization (within 60 s). Data are mean + s.e.m. from 4 to 6 experiments performed in duplicate. (a) Calhex231 retains PAM activity, and can negatively regulate its own activity, at an N-terminally truncated CaSR (NT-trunc). (b) Calhex231-mediated positive and negative modulation of Ca^{2+}_o-mediated Ca^{2+}_i mobilization is lost at Glu837$^{7.32}$Ile (E837I). (c,d) Negative but not positive modulation of Ca^{2+}_o-mediated Ca^{2+}_i mobilization by calhex231 is abolished at Phe688$^{3.40}$Ala (F688A; c) or Ile841$^{7.36}$Ala (I841A; d). (e,f) Negative modulation of AC265347-mediated Ca^{2+}_i mobilization by calhex231 is significantly attenuated at Phe688$^{3.40}$Ala (F688A; e) or Ile841$^{7.36}$Ala (I814A; f). (g,h) Arg680$^{3.32}$Ala (R680A) selectively abolishes calhex231-mediated positive modulation of Ca^{2+}_o (g) but calhex231-mediated negative modulation of Ca^{2+}_o (g) and AC265347 (h) are retained. Curves in panel a are the best fit to eq 2. Curves in b,e,f are the best fit to eq 1, where parameters describing the curves are shown in Supplemental Table 6. Curves in c,d and g,h are the best fit to eqs 3 or 4, respectively, where parameters describing the curves are shown in Table 1. Direction and magnitude of arrows demonstrate the influence of calhex231 on agonist pEC_{50} or E_{max}, with mixed mode activity denoted by a U-turn arrow.

Table 1. Calhex231 Affinity (pK_B), Binding Cooperativity ($\log\alpha$), Efficacy Cooperativity ($\log\beta$) or a Composite Cooperativity Value ($\log\alpha\beta$) at the WT and Mutant CaSRs[a]

	Ca^{2+}_o versus calhex231			AC265347 versus calhex231			
	pK_B	$\log\alpha\beta$ ($\alpha\beta$)	n	pK_B	$\log\alpha$ (α)	$\log\beta$ (β)	n
WT	ND	ND	6	6.51 ± 0.10	−0.53 ± 0.12 (0.3)	−0.92 ± 0.14 (0.1)	5
NT-trunc.	ND	ND	3	7.39 ± 0.11[b]	−1.07 ± 0.14[b] (0.09)	−1.23 ± 0.19 (0.06)	3
F668A	5.29 ± 0.33[b]	≈−100 (≈0)[c]	4	6.38 ± 0.19	≈−100 (≈0)	0 (1)[d]	3
R680A	4.10 ± 0.05[b]	≈−100 (≈0)[c]	4	6.72 ± 0.11	−1.03 ± 0.25 (0.09)	≈−52 (≈0)[c]	3
F684A	>5	NCA	5	NAA	NAA	NAA	2
F688A	5.94 ± 0.07	0.51 ± 0.02 (3.2)	6	NCA	NCA	NCA	4
E767A	5.05 ± 0.09[b]	≈−100 (≈0)[c]	4	7.24 ± 0.14[b]	−0.42 ± 0.13 (0.4)	−1.79 ± 0.31[b] (0.02)	3
W818A	NCA	NCA	4	NAA	NAA	NAA	2
F821A	6.55 ± 0.07	−0.03 ± 0.002 (0.93)	4	7.34 ± 0.13[b]	−0.67 ± 0.15 (0.2)	−0.37 ± 0.05 (0.4)	4
E837I	NCA	NCA	3	NAA	NAA	NAA	4
I841A	6.04 ± 0.34	0.16 ± 0.03 (1.4)	4	NCA	NCA	NCA	4
cmyc-CaSR(908)$_{B1}$ + Flag-CaSR(F801A E837I 908)$_{B2}$	5.91 ± 0.40	0.26 ± 0.06 (1.8)	3	NP	NP	NP	

[a] Ca^{2+}_o-mediated Ca^{2+}_i mobilization was determined in the absence and presence of a range of Ca^{2+}_o and calhex231 concentrations in 0.1 mM ambient Ca^{2+}_o using a pre-incubation paradigm, and data were fitted to an operational model of allosterism (equation 2). Data are mean ± s.e.m. from pooled experiments performed in duplicate. Notation: ND, not determined due to mixed PAM and NAM activity; NCA, no or weak calhex231 activity; NAA, no or weak AC265347 activity; NP, not performed; ≈, approaching. [b] Significantly different to WT determined in AC265347 versus calhex231 interaction studies, $p < 0.05$, one-way ANOVA with Dunnett's multiple comparisons. [c] The magnitude of negative cooperativity is so great that it is approaching 0 (≈0) and cannot be accurately quantified. [d] Logβ (efficacy cooperativity) was fixed to 0 due to no calhex231 modulation of agonist E_{max}.

We evaluated the effects of each mutation on the ability of calhex231 to modulate the function of Ca^{2+}_o, which binds both the VFT and 7TM domain, and AC265347, which binds exclusively in the 7TM domain. We first sought to determine calhex231 affinity (pK_B) at the WT CaSR by fitting the AC265347 versus calhex231 interaction data to an operational model of allosterism, (eq 3; Table 1). We next tested the impact of mutations within the CaSR's 7TM domain on the ability of calhex231 to modulate Ca^{2+}_o or AC265347-mediated Ca^{2+}_i mobilization. Ala substitution of Trp818$^{6.50}$ or Ile

DOI: 10.1021/acsptsci.8b00021
ACS Pharmacol. Transl. Sci. 2018, 1, 96−109

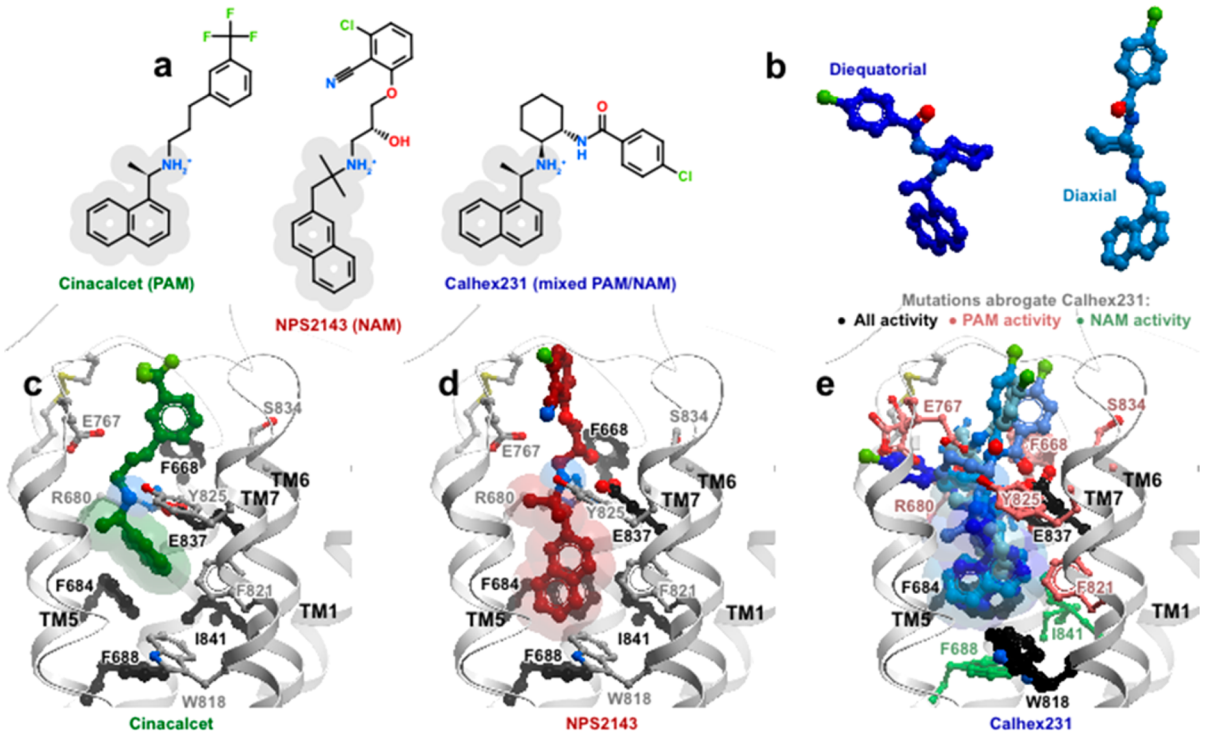

Figure 5. Cinacalcet, NPS2143, and calhex231 bind to a common arylalkylamine 7TM domain binding site. (a) Structures of cinacalcet, NPS2143, and calhex231, with shading highlighting their naphthylamine moiety. (b) The *trans*-1,2-disubstituted cyclohexane ring of calhex231 can adopt diequatorial or diaxial conformations, resulting in bent or extended calhex231 conformations, respectively. (c–e) Cinacalcet, NPS2143, and calhex231 activity are dependent on key amino acid residues that line an extended 7TM domain cavity, and their binding is restrained by a salt bridge between the protonated arylalkylamine secondary amine and Glu837$^{7.32}$ in TM7. Residues shown are those where mutations abrogate calhex231 PAM activity (red in panel c), NAM activity (green in panel c), or both (black in panel c). Residues where mutations attenuate cinacalcet and NPS2143 affinity are also shown in black in panels a and b. Whereas docking studies predict cinacalcet (a) and NPS2143 (b) adopt an extended binding pose with the substituted phenyl pointing up toward the VFT domain (not shown in model), calhex231 (c) is predicted to assume a "bent" or "extended" conformation depending on whether its *trans*-1,2-disubstituted cyclohexane ring adopts an diequatorial or diaxial conformation, respectively. Consequently, the substituted phenyl of calhex231 may point up toward the VFT domain (diaxial) or is buried in the top of the TM domains and bottom of the ECLs (diequatorial). These docking studies suggest calhex231 is structurally more flexible than NPS2143 and cinacalcet, and therefore has a greater propensity to adopt at least two distinct poses within the common 7TM binding pocket.

substitution of Glu837$^{7.32}$ resulted in a reduction in calhex231 activity, evidenced by a complete loss (Glu837$^{7.32}$Ile) or a reduction in the magnitude (Trp818$^{6.50}$Ala) of effect on Ca^{2+}_o potency or E_{max}, respectively (Figure 4b, Supplemental Figure 2a and Supplemental Table 6). We were unable to perform AC265347 versus calhex231 interaction experiments at Trp818$^{6.50}$Ala and Glu837$^{7.32}$Ile mutants, because AC265347 had diminished affinity, rendering it unable to stimulate sufficient Ca^{2+}_i mobilization.[4] Nonetheless, the loss in calhex231 modulation of Ca^{2+}_o by mutations that also reduce NPS2143 and/or cinacalcet affinity is consistent with the known contribution of these residues to the arylalkylamine binding pocket.[4]

Interestingly, Ala substitution of Phe684$^{3.36}$, Phe688$^{3.40}$, and Ile841$^{7.36}$ completely abolished calhex231-mediated negative modulation of Ca^{2+}_o, but the PAM activity was retained (Figure 4c,d Supplemental Figure 2b, Supplemental Table 6). Quantification with an allosteric model (equation 4) revealed that the calhex231 pK_B was reduced at Phe684$^{3.36}$Ala in comparison to the pK_B determined in interaction studies versus AC265347 at the WT CaSR (Table 1). In contrast, calhex231 pK_B was not significantly affected by the Phe688$^{3.40}$Ala or Ile841$^{7.36}$Ala mutations (Table 1). We were again unable to perform AC265347 versus calhex231 interaction experiments at the Phe684$^{3.36}$Ala mutant, because AC265347 has diminished affinity.[4] However, calhex231 NAM activity against AC265347 was significantly attenuated at Phe688$^{3.40}$Ala or Ile841$^{7.36}$Ala, with a small reduction in AC265347 potency and E_{max} observed only in the presence of 10 μM calhex231 (Figure 4e,f). Collectively, these findings indicate that calhex231 inhibition of Ca^{2+}_o or AC265347 depends on Phe688$^{3.40}$, whereas calhex231 potentiation of Ca^{2+}_o does not require this residue, thus suggesting calhex231 may mediate positive and negative modulation from two distinct binding sites.

Contrary to the Phe684$^{3.36}$Ala, Phe688$^{3.40}$Ala, or Ile841$^{7.36}$Ala mutations, positive modulation of Ca^{2+}_o by calhex231 was completely abolished at Phe668$^{2.56}$Ala, Arg680$^{3.32}$Ala, Glu767^{ECL2}Ala, or Phe821$^{6.53}$Ala, but calhex231 retained its negative modulation of Ca^{2+}_o and AC265347 at these mutants (Figure 4g,h, Supplemental Figure 2c–h, Supplemental Table 6). Fitting the AC265347/calhex231 interaction data to the operational model of allosterism revealed that Glu767^{ECL2}Ala or Phe821$^{6.53}$Ala increased calhex231 pK_B, whereas Phe668$^{2.56}$Ala or Arg680$^{3.32}$Ala had no significant effect (Table 1). However, when we fitted Ca^{2+}_o versus calhex231 interaction data to the operational model of allosterism, the estimated pK_B at all these mutants was significantly lower than the pK_B calculated when AC265347 was the activating probe (Table 1), indicating a potential

DOI: 10.1021/acsptsci.8b00021
ACS Pharmacol. Transl. Sci. 2018, 1, 96–109

difference in mechanism of calhex231 modulation of the different probes (see below).

At Tyr825$^{6.57}$Ala, Val833^{ECL3}Ala, or Ser834^{ECL3}Ala CaSR mutants, modulation mediated by calhex231 was still apparent, but there was a reduction in the extent of, or loss of, positive modulation at Tyr825$^{6.57}$Ala or Ser834^{ECL3}Ala, respectively (Supplemental Figure 2i–k, Supplemental Table 6). We did not further investigate the ability of calhex231 to modulate AC265347 activity at these mutants.

Collectively, these mutagenesis data support the hypothesis that calhex231 binds to the 7TM binding site utilized by other arylalkylamine PAMs and NAMs.[4,6−8] However, the mixed PAM and NAM activity exhibited by calhex231, the ability of specific mutations to selectively abolish PAM activity while retaining NAM activity, and vice versa, and differences in calhex231 affinity at these mutants depending on the selection of probe (Ca^{2+}_o or AC265347), suggests that calhex231-mediated allostery is not consistent with a ternary complex model mediated by a single allosteric site. Rather, this type of behavior is only possible where two distinct binding sites are operative at different calhex231 concentrations.

Calhex231 Binds in the Arylalkylamine Binding Pocket. To better interpret the concentration-dependent cooperativity switch of calhex231 at the WT CaSR, as well as differential effects of mutations on cooperativity and affinity, we docked calhex231 into a homology model of the CaSR based on the $mGlu_5$ 7TM crystal structure.[20] As comparators, we also docked the arylalkylamines, NPS2143 (NAM) and cinacalcet (PAM). Notably, in all known arylalkylamine CaSR PAMs and NAMs, the topology of the ligand core dictates PAM versus NAM activity. For instance, naphthylethylamines (e.g., cinacalcet[21] and calindol[22]) exhibit PAM activity, whereas naphthyl- or indanylpropylamines (e.g., NPS2143[23] and ronacaleret,[24] respectively) are NAMs. Calhex231, however, constitutes an exception; its structure is consistent with the naphthylethylamine PAMs (Figure 5a) but, as we have shown herein, it is a mixed PAM/NAM. In contrast to NPS2143 and cinacalcet, calhex231 possesses a flexible *trans*-1,2-disubstituted cyclohexane ring, which may adopt multiple conformations ranging from diequatorial to diaxial based on the orientation of nitrogen atoms at these positions. The lowest energy conformer of the ring is a "chair" with diequatorial attachments followed by a "chair" with diaxial attachments[25,26] (Figure 5b), and interconversion of the two is possible at physiological temperatures. To account for this interconversion, docking studies were performed with both calhex231 conformations.

Representative poses for cinacalcet, NPS2143, and calhex231 are shown in Figure 5c–e. Consistent with our previous modeling, both cinacalcet (Figure 5c) and NPS2143 (Figure 5d) predominantly adopted an extended conformation, and docked in the space that spanned from the middle of the 7TM cavity to the ECLs. The naphthyl cores of both molecules favorably packed among the aromatic and aliphatic residues at the center of the 7TM cavity (e.g., Phe684$^{3.36}$, Ile841$^{7.36}$, and Trp818$^{6.50}$), and the charged secondary amine formed a salt bridge with Glu837$^{7.32}$. The 7TM cavity hydrophobic packing and the salt bridge with Glu837$^{7.32}$ were also observed in the case of calhex231 (Figure 5e); however, an extended conformation is only achievable for the diaxial conformer of calhex231, whereas the diequatorial conformer preferentially adopts a bent pose with the chlorophenyl buried among the junction of TM3/ECL1 and TM5/ECL2 rather than pointing upward toward the VFT (absent in the models). Notably, this diequatorial bent pose resembled the previously solved crystal structure of a calhex231 analogue in solution.[10] The conformational diversity of calhex231 also allowed for greater diversity in the position of its naphthyethylamine motif with respect to the key residues mediating ligand binding and cooperativity (Figure 4e).

To probe the possibility that calhex231 may adopt multiple binding poses due to its flexible *trans*-1,2-disubstituted cyclohexane ring, we performed Ca^{2+}_o/calhex231 interaction studies in CaSR-HEK293 cell Ca^{2+}_i mobilization assays at 25 °C; 12 °C lower than the physiological 37 °C used in our prior studies. The diaxial *trans*-1,2-disubstituted cyclohexane conformation is energetically less favorable than the diequatorial conformation. A reduction in thermodynamic energy may therefore shift the equilibrium toward the energetically favored diequatorial *trans*-1,2-disubstituted cyclohexane conformation. At 25 °C, 10 μM calhex231 mediated significantly greater (2.6-fold) inhibition of Ca^{2+}_o signaling in comparison to its effect at 37 °C, suggesting that calhex231 was a better NAM at the lower temperature (Supplemental Figure 3a). In contrast, inhibition mediated by NPS2143 was unaffected by temperature (Supplemental Figure 3b). Thus, calhex231 may have greater flexibility than the other arylalkylamines when bound within the 7TM cavity, accounted for by conformational variability in its *trans*-1,2-disubstituted cyclohexane ring.

Calhex231 Mediates Allostery Across a Dimer. Our mutagenesis studies indicated that certain mutations selectively abolished calhex231 NAM activity at the exclusion of PAM activity, and vice versa. These findings suggest that distinct amino acid residues mediate calhex231 PAM activity at the exclusion of NAM activity, and vice versa, which could be indicative of calhex231 mediating its different effects via two distinct binding sites. However, all the mutations studied herein are located in the arylalkylamine binding site, and our computational modeling suggested that calhex231 bound within this site, albeit perhaps with more conformational flexibility than NPS2143 or cinacalcet. If calhex231 were to mediate both positive and negative modulation of Ca^{2+}_o signaling from the same binding site, it would sterically hinder its own binding. Therefore, a mixed mode of allostery arising from a similar binding pocket can only be reconciled if calhex231 modulates CaSR activity across a dimer. Indeed, a previous study revealed that NAMs must bind to both protomers in a CaSR dimer to mediate their full inhibitory effects.[27] However, our findings are the first to suggest that an allosteric modulator can switch from a PAM to a NAM depending on its occupancy of one versus two protomers in the dimer. This hypothesis is consistent with our findings at the N-terminally truncated CaSR, which, based on findings at other N-terminally truncated Class C GPCRs,[28] would be expected to have a lower propensity to dimerize and where calhex231 NAM activity was lost. Similarly, a recent study indicated that NPS2143 inhibition of the CaSR was reduced when it was only able to occupy a single protomer in a dimer.[27]

To more directly test the hypothesis that calhex231 mediates its mixed mode of allostery across a dimer, we took advantage of a unique feature of the Class C GPCR gamma-aminobutyric acid receptor subtypes B1 and B2 ($GABA_{B1}$ and $GABA_{B2}$). Specifically, each $GABA_B$ subunit contains approximately 30 amino acid residues within their C-terminus that mediate $GABA_{B1}$ and $GABA_{B2}$ heterodimerization via a high affinity coiled-coil interaction between the C-terminal tails.[29] In

DOI: 10.1021/acsptsci.8b00021
ACS Pharmacol. Transl. Sci. 2018, 1, 96−109

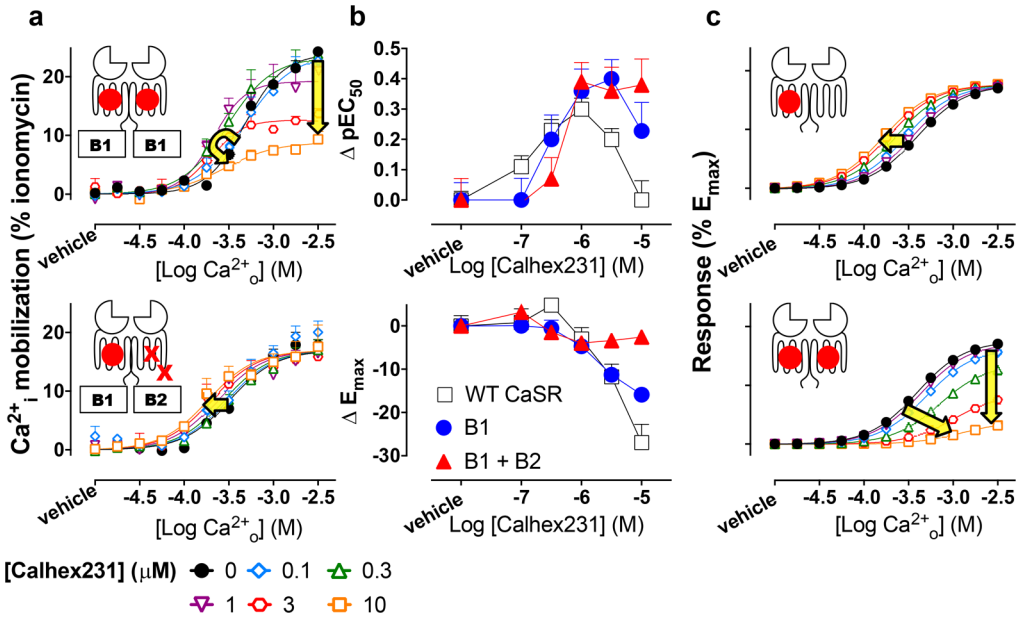

Figure 6. Calhex231 mixed PAM and NAM activity is consistent with allostery across a dimer. (a) Calhex231 retains mixed PAM and NAM activity at cmyc-CaSR(908)$_{B1}$ expressed alone (top panel), but becomes a pure PAM when cmyc-CaSR(908)$_{B1}$ heterodimerizes with the signaling- and calhex231 binding-impaired Flag-CaSR(F801A E837I 908)$_{B2}$ (bottom panel); cmyc-CaSR(908)$_{B1}$ signaling following transient expression in FlpIn HEK293 cells alone or in combination with Flag-CaSR(F801A E837I 908)$_{B2}$ Ca^{2+}_o-mediated Ca^{2+}_i mobilization in the absence or presence of calhex231 was determined in 0.1 mM ambient Ca^{2+}_o, following a 20 min calhex231 preincubation prior to determination of peak agonist-mediated Ca^{2+}_i mobilization (within 60 s). Data are mean + s.e.m. from 3 experiments performed in duplicate. Curves in panel a are the best fit to equation 1, and parameters describing the curves are shown in Supplemental Table 7. Curves in panel b are the best fit to equation 4, and parameters describing the curves are shown in Table 1. (b) Calhex231-mediated changes in Ca^{2+}_i potency (pEC_{50}) (top panel) and E_{max} (bottom panel) at the WT CaSR, cmyc-CaSR(908)$_{B1}$ homodimer (B1) or cmyc-CaSR(908)$_{B1}$/Flag-CaSR(F801A E837I 908)$_{B2}$ heterodimer (B1 + B2), following determination of Ca^{2+}_o-mediated Ca^{2+}_i mobilization in the absence or presence of calhex231 as described for panel a. (c) Schematic of calhex231 actions at the CaSR, summarizing its mixed PAM and NAM activity. When calhex231 binds to only one protomer in a CaSR dimer, it is a PAM, but when it binds to both protomers, it is a NAM. Cartoons in panel a depict the function of the cmyc-CaSR(908)$_{B1}$ and Flag-CaSR(F801A E837I 908)$_{B2}$ constructs, where the red circle indicates that cmyc-CaSR(908)$_{B1}$ can bind calhex231 and the red crosses indicate that Flag-CaSR(F801A E837I 908)$_{B2}$ cannot bind calhex231 and cannot signal due to the E837I and F801A mutations, respectively. Cartoons in panel c depict the functional receptor unit that gives rise to the response shown in the graph, where the red circle indicates which protomers bind calhex231. Direction and magnitude of arrows demonstrate the influence of calhex231 on agonist pEC_{50} or E_{max}, with mixed mode activity denoted by a U-turn arrow.

contrast homodimers between the GABA$_{B1}$ C-terminus are relatively unstable, and do not reach the cell surface due to the presence of an endoplasmic reticulum retention motif that is masked upon heterodimerization with GABA$_{B2}$.[30,31] We thus generated two CaSR constructs in which the last 170 CaSR residues (909−1078) were replaced with the last 107 or 182 residues of GABA$_{B1}$ or GABA$_{B2}$, respectively. The GABA$_{B1}$ residues were introduced into a cmyc-tagged CaSR, referred to herein as "cmyc-CaSR(908)$_{B1}$", and the GABA$_{B2}$ residues were introduced into a Flag-tagged CaSR that contained two mutations: Phe801^{ICL3}Ala, which impairs CaSR signaling;[27] and Glu837$^{7.32}$Ile, which abolishes calhex231 binding (Figure 4b). The latter construct is herein referred to as "Flag-CaSR(F801A E837I 908)$_{B2}$". If cmyc-CaSR(908)$_{B1}$ were to heterodimerize with Flag-CaSR(F801A E837I 908)$_{B2}$, the resultant dimer would consist of one in which both protomers can bind calcium, but only the cmyc-CaSR(908)$_{B1}$ protomer can bind calhex231 and signal.

We first measured the cell surface expression of the cmyc-CaSR(908)$_{B1}$ and Flag-CaSR(F801A E837I 908)$_{B2}$ constructs using flow cytometry analysis following transient expression of either construct alone or together. When expressed alone, cmyc-CaSR(908)$_{B1}$, and to a lesser degree, Flag-CaSR(F801A E837I 908)$_{B2}$ expression was significantly reduced in comparison to WT (~20% and 50% WT, respectively) (Supplemental Figure 4a). When coexpressed together, CaSR(908)$_{B1}$ surface expression was significantly increased (to ~40% WT), and Flag-CaSR(F801A E837I 908)$_{B2}$ expression decreased (~30% WT), suggesting that the two receptors altered one another's surface expression, most likely via heterodimerization.

We next sought to evaluate allosteric modulation of Ca^{2+}_o-mediated Ca^{2+}_i mobilization by calhex231 at the cmyc-CaSR(908)$_{B1}$ and Flag-CaSR(F801A E837I 908)$_{B2}$ constructs expressed alone or together. Ca^{2+}_o stimulated Ca^{2+}_i mobilization at cmyc-CaSR(908)$_{B1}$, and calhex231 retained its mixed PAM/NAM activity, much like at the WT CaSR (Figure 6a top panel, 6b). As expected, Ca^{2+}_o was unable to stimulate Ca^{2+}_i mobilization at Flag-CaSR(F801A E837I 908)$_{B2}$ and calhex231 also demonstrated no activity (Supplemental Figure 4b). Importantly, when cmyc-CaSR(908)$_{B1}$ and Flag-CaSR(F801A E837I 908)$_{B2}$ were coexpressed together, Ca^{2+}_o-mediated Ca^{2+}_i mobilization was similar to that observed at the cmyc-CaSR(908)$_{B1}$ expressed alone, but calhex231 became a pure PAM (Figure 6a bottom panel, 6b; Supplemental Table 7). We fitted this calhex231-mediated positive modulation of Ca^{2+}_o to an operational model of allosterism (equation 4), revealing the calhex231 pK_B to be similar to its pK_B determined at the WT CaSR when AC265347 was the probe (Table 1). This finding directly demonstrates that the cmyc-CaSR(908)$_{B1}$

DOI: 10.1021/acsptsci.8b00021
ACS Pharmacol. Transl. Sci. 2018, 1, 96−109

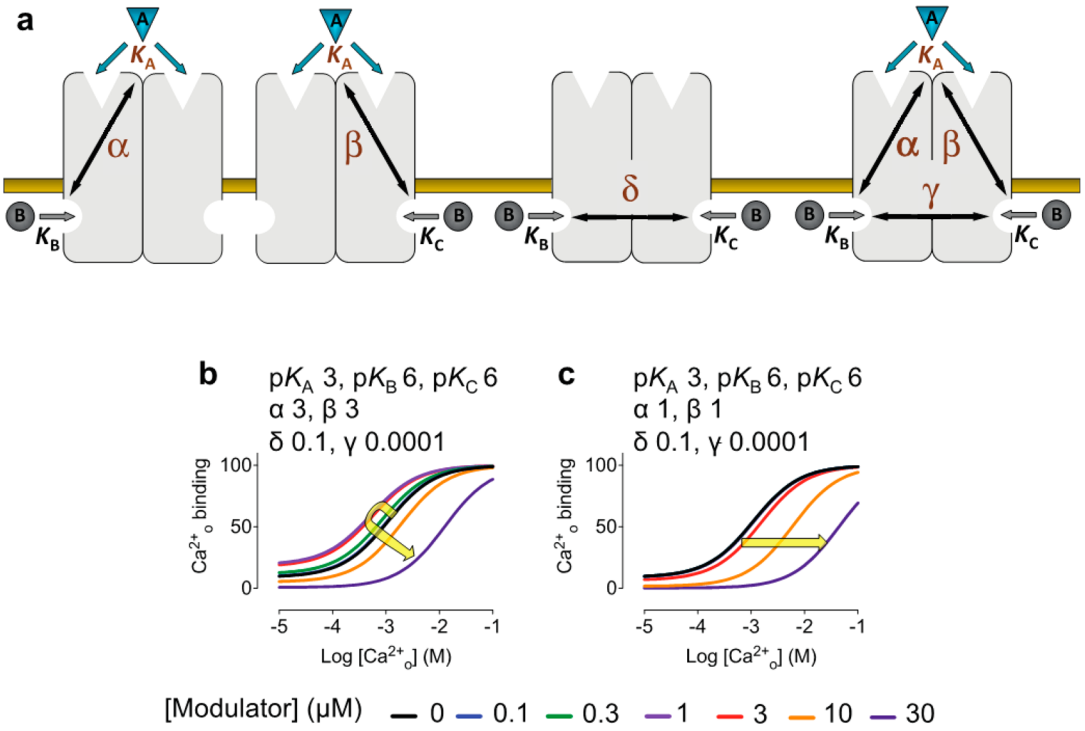

Figure 7. Calhex231 mixed PAM and NAM activity can be described by an allosteric quaternary complex model. (a) An allosteric quaternary complex model describes the interaction between an orthosteric agonist and an allosteric modulator that binds to two binding sites (e.g., two protomers in a dimer). When the allosteric modulator binds to either one of the two allosteric binding sites with an equilibrium dissociation constant (affinity), K_B or K_C, it alters the binding affinity of the orthosteric agonist (K_A) via the cooperativity factors, α and β, respectively. The interaction between the allosteric modulator and itself is driven by the cooperativity factor δ in the absence of orthosteric agonist, and by the cooperativity factor γ in the presence of orthosteric agonist. (b) Simulations with the allosteric quaternary complex model indicate that mixed PAM and NAM activity can occur when the modulator binds to both allosteric binding sites with the same affinity and positively modulates orthosteric agonist binding via both sites, if there is a significant negative interaction between the modulator and itself in the presence of the orthosteric agonist. (c) When a modulator has neutral cooperativity with the orthosteric agonist (i.e., α and $\beta = 1$), but negative cooperativity with itself when the orthosteric agonist is bound (e.g., $\gamma = 0.0001$), the modulator appears to be a low affinity negative modulator of orthosteric agonist binding. This resembles the effects of calhex231 at "PAM-null" mutant CaSRs. Direction and magnitude of arrows demonstrate the influence of the modulator on agonist pEC_{50} or E_{max}, with mixed mode activity denoted by a U-turn arrow.

and CaSR(F801A E837I 908)$_{B2}$ form a CaSR heterodimer at which calhex231 can only act as a PAM because it can only bind to the one functional protomer in the dimer, consistent with our hypothesis that calhex231 is a PAM when bound to one protomer, and a NAM when bound to two. This is summarized in Figure 6c.

To further establish how calhex231 could behave as a PAM or NAM depending on how many protomers in the CaSR dimer it occupies, we performed mathematical simulations of the effect of a modulator that binds to two sites on the binding of an orthosteric agonist using a modified version of an allosteric quaternary complex model[32] (equation 5; Figure 7a). In this model, K_A is the affinity (dissociation constant) of the orthosteric agonist; the affinity of the allosteric modulator is K_B at site 1 and K_C at site 2. Four different parameters describe allosteric cooperativity within the model. α and β describe the cooperativity between orthosteric agonist and allosteric modulator bound to sites 1 and 2, respectively. δ denotes the cooperativity between the two allosteric sites when the orthosteric agonist is absent, whereas γ is the cooperativity between the two allosteric sites when the receptor is simultaneously bound with orthosteric agonist.

Simulations closely recapitulating our experimental findings indicated that apparent mixed PAM and NAM activity could arise when the modulator was a PAM of orthosteric agonist binding from both modulator binding sites (i.e., α and $\beta > 1$), but when there was a negative interaction between the two modulator binding sites in the presence of the orthosteric agonist (i.e., $\gamma < 1$) (Figure 7b). Due to the reciprocal nature of allosteric binding interactions, when $\gamma < \delta$, orthosteric agonist binding is reduced when the modulator occupies both allosteric binding sites (e.g., at high modulator concentrations). This model is consistent with recent findings indicating that whereas PAMs need only occupy a single protomer of a CaSR dimer to potentiate receptor signaling, NAMs must occupy both protomers to achieve their maximum inhibitory capabilities.[27] We tested this concept at the N-terminally truncated CaSR, which has reduced Ca^{2+}_o occupancy due to removal of the primary VFT Ca^{2+}_o binding sites. Indeed, interaction studies between calhex231 and AC265347 at the N-terminally truncated CaSR indicated that the calhex231 pK_B was almost 30-fold higher than at the WT receptor (Table 1).

Further support for this model came from simulations showing that when α and β are neutral, the modulator behaves as a lower affinity NAM (Figure 7c), much like the activity of calhex231 at the "PAM-null" mutant receptors, Arg680$^{3.32}$Ala or Glu767^{ECL2}Ala. Similarly, a reduction in the difference between the values of δ and γ (e.g., δ and γ are equal to one another) recapitulates the "NAM-null" mutant, Phe688$^{3.40}$Ala;

DOI: 10.1021/acsptsci.8b00021
ACS Pharmacol. Transl. Sci. 2018, 1, 96−109

that is, there is a loss in cooperativity between the two modulator binding sites in the presence of the orthosteric agonist, or an increase in negative cooperativity between the modulator binding sites in the absence of the orthosteric agonist.

Of note, an alternative model could also recapitulate mixed PAM and NAM activity when the modulator mediates positive and negative cooperativity with the orthosteric agonist from the two different binding sites (e.g., $\alpha > 1$, $\beta < 1$), but only when the modulator's pK_B at the "PAM" site (site 1) is higher than its pK_C at the "NAM" site (site 2). However, this is inconsistent with our experimental findings that the calhex231 pK_B for the "NAM-null" mutants, Phe688$^{3.40}$Ala or Ile841$^{7.36}$Ala, is similar to that for the WT CaSR (Table 1), and it does not explain observed pK_B differences at mutant CaSRs with the use of different agonist probes.

DISCUSSION

The current study reveals, for the first time, a novel mechanism of allosteric "mode-switching" at a Class C GPCR. By combining an in-depth analysis of allosteric modulation with mutagenesis, analytical pharmacology, computational modeling, and mathematical simulations, we reveal that the previously reported "NAM", calhex231, mediates both positive and negative allosteric modulation in a CaSR dimer, depending on its concentration and site(s) of interaction. As such, nonsaturating concentrations of calhex231 act to positively modulate the orthosteric CaSR agonist, Ca^{2+}_o, by binding to a single protomer at a time, while concentrations that saturate both protomers of a dimer inhibit Ca^{2+}_o activity. Importantly, we demonstrate that this allosteric mode switching occurs at CaSRs endogenously expressed in parathyroid gland cells, and where calhex231 suppresses (PAM activity) or stimulates (NAM activity) PTH release.

For many GPCRs, ligand-mediated inhibition of receptor signaling can be achieved by receptor downregulation (e.g., phosphorylation, internalization). We considered this phenomenon as a possible explanation for the observed NAM activity of high concentrations of calhex231, and believe it to be unlikely for the following reasons: (i) previous studies indicate CaSR cell surface expression is not reduced upon agonist or PAM exposure, and indeed calhex231 had no significant effect on cell surface CaSR expression in the present study; (ii) calhex231 exhibited NAM activity in the presence of a PKC inhibitor, suggesting calhex231 does not potentiate PKC-mediated CaSR desensitization; (iii) unlike cinacalcet, calhex231 did not deplete Ca^{2+}_i stores by potentiating ambient Ca^{2+}_o in the assay buffer; (iv) receptor desensitization is not consistent with estimated differences in calhex231 affinity in the presence of different agonist probes. In view of this, the most parsimonious explanation for the unique mixed PAM/NAM action of calhex231 is allostery in a CaSR dimer. This explanation is fully supported by our findings that calhex231 was a pure PAM at a CaSR heterodimer consisting of one fully functional protomer (cmyc-CaSR(908)$_{B1}$) and a signaling- and calhex231 binding-impaired protomer (Flag-CaSR(F801A E837I 908)$_{B2}$.

Our findings support a proposed model of Class C GPCR allosteric modulation indicating that a PAM can achieve its maximal positive modulation by binding to only a single protomer in a dimer, whereas NAMs must bind to both protomers to attain their capacity to inhibit receptor activation.[27,33,34] The mixed allosteric activity of calhex231 is also reminiscent of previous findings at the CaSR and mGlu receptors, where PAMs can artificially switch to NAMs when bound exclusively to a mutated protomer that cannot activate G proteins,[27,33] indicating that activation of one protomer's 7TM domain inhibits the 7TM of the other protomer. Calhex231, however, is unique in being the only modulator identified to date that undergoes concentration-dependent mode-switching at a WT Class C GPCR under normal physiological conditions. Importantly, this unique mode of allostery enables calhex231 to fully inhibit CaSR signaling in HEK293 cells, whereas the prototypical NAM, NPS2143, only partially inhibits signaling. The ability of calhex231 to completely "switch off" the CaSR in HEK293 cells (albeit at high concentrations) could provide a new avenue to design CaSR NAMs for therapeutic purposes where this would be desirable. For instance, NAMs that completely block CaSR signaling may be more efficient at stimulating PTH release to stimulate bone formation in osteoporosis, although we were unable to test such high calhex231 concentrations in our PTH release assay due to unfeasible amounts of compound required. On the contrary, if the modulator is a mixed PAM/NAM, when *in vivo* drug concentrations drop, the modulator will activate rather than inhibit the CaSR.

Consistent with previous predictions that calhex231 binds to a site that overlaps with that utilized by cinacalcet and NPS2143,[7,8] our data indicate that calhex231 PAM and NAM activity are significantly attenuated by Ala substitution of Phe684$^{3.36}$ or Trp818$^{6.50}$, or Ile substitution of Glu837$^{7.32}$, reminiscent of the reduction in cinacalcet and/or NPS2143 binding at these mutants.[4] This is unsurprising given that calhex231 possesses a naphthalene group and a central amine akin to those of cinacalcet and NPS2143 that are predicted to interact with these residues.[4] However, computational modeling suggests that the "flip" in calhex231 activity may be related to conformational heterogeneity in calhex231 binding, facilitated by the flexible *trans*-1,2-disubstituted cyclohexane ring present in calhex231, but not other arylalkylamines. The distinct conformations adopted by calhex231 enable it to allosterically modulate itself across the dimer when the receptor is simultaneously occupied by Ca^{2+}_o. Due to the reciprocal nature of allosteric interactions, this results in a concomitant reduction in Ca^{2+}_o binding and/or signaling when calhex231 occupies both protomers. An allosteric quaternary complex model explains how this may occur. Mixed PAM and NAM activity can arise if calhex231 is a PAM of orthosteric agonist binding from both protomer binding sites via the cooperativity factors α and β, but negatively modulates its own binding in the presence of Ca^{2+}_o via the cooperativity factor γ. As allosteric and orthosteric binding interactions are reciprocal, this means that calhex231 also reduces Ca^{2+}_o binding via the cooperativity factor γ. Differences in the cooperativity factors for NPS2143, on the other hand, may result in a weaker effect on Ca^{2+}_o (e.g., γ is neutral and NPS2143 effects on Ca^{2+}_o binding are driven purely by α and/or β).

Our study also indicates that CaSR allostery can be context-dependent, with calhex231 behavior depending on the concentration of ambient Ca^{2+}_o and on the assay paradigm used to detect its allosteric modulation, highlighting that prior CaSR NAM drug discovery approaches may have resulted in misinterpretation of allosteric modulator activity. Replotting data in Figure 1a and 1b (shown in Supplemental Figure 5) reveals why the mixed PAM and NAM activity of calhex231

DOI: 10.1021/acsptsci.8b00021
ACS Pharmacol. Transl. Sci. 2018, 1, 96−109

may have been missed in the original description of this compound; if a maximally activating Ca^{2+}_o concentration is employed (much like the E_{max} concentration used in the original paper[8]), calhex231 appears to be a pure NAM. Its mixed PAM and NAM activity only becomes apparent when lower Ca^{2+}_o concentrations are used.

Further, as is observed for many GPCRs including those belonging to Class C,[3] calhex231 cooperativity is also probe-dependent, which has significant implications for the use of surrogate agonists for CaSR drug discovery efforts. These findings have major implications for informing future rational screening for CaSR NAMs. In conclusion, the current study provides new insight into a novel mode of CaSR allosteric modulation and mode-switching that is physiologically relevant, and can facilitate future drug discovery efforts that seek to target the CaSR with allosteric drugs.

MATERIALS AND METHODS

FlpIn TREx Human Embryonic Kidney (HEK) 293 cells, Dulbecco's Modified Eagle's Medium (DMEM), blasticidin S HCl, fetal bovine serum (FBS), Fluo-4-AM, and Sytox Blue (Molecular Probes) were obtained from Invitrogen (Carlsbad, CA, USA), whereas hygromycin B was from Roche (Mannheim, Germany). Polyethylenimine (PEI) Max (MW 40K) was purchased from Polysciences Inc. (Pennsylvania, USA). Calhex231 hydrochloride (4-chloro-*N*-[(1*S*,2*S*)-2-[[(1*R*)-1-(1-naphthalenyl)ethyl]amino]cyclohexyl]-benzamide hydrochloride) was obtained from Tocris Bioscience (Bristol, United Kingdom) and was validated as a pure calhex231 sample in-house using QC LCMS. AF647-conjugated 9E10 antibody was made in-house as described previously.[14] Tetracycline HCl, propidium iodide, FITC-conjugated anti-Flag antibody and other general reagents were purchased from Sigma-Aldrich (St. Louis, MI, USA).

Generation of cmyc-CaSR(908)$_{B1}$ and Flag-CaSR-(F801A E837I 908)$_{B2}$. The last 107 amino acid residues of the mouse $GABA_{B1}$ C-terminus (residues 854−960; NP_062312.3) or the last 182 amino acid residues of the human $GABA_{B2}$ C-terminus (residues 760−941; NP_005449.5) were PCR amplified from $GABA_{B1}$ or $GABA_{B2}$ cDNA, respectively (a kind gift from Prof David Hampson, University of Toronto, Canada) with a forward primer encoding a 5′ *Bam*HI site (5′actgactgggatccgacaccatgaagacagggtc) and a reverse primer encoding a 3′ *XbaI* site (3′atcgatcgtctagatcacttataaagcaaatgca). A natural *Bam*HI restriction site (GGA TCC) is present in the CaSR at codons 2719−2724, which encodes residues G907 and S908 in the CaSR protein. Therefore, cmyc-CaSR in pcDNA5/frt/TO (described previously[14]) was digested with *Kpn*I and *Bam*HI and the resultant fragment and the $GABA_{B1}$(854−960) PCR product were separately ligated with pcDNA3.1+ digested with *Kpn*I and *Bam*HI (for cmyc-CaSR(1−908) ligation) or *Bam*HI and *XbaI* (for $GABA_{B1}$(854−960) ligation) to generate cmyc-CaSR(1−908)-$GABA_{B1}$(854−960) (referred to herein as cmyc-CaSR(908)$_{B1}$). pcDNA3.1+ containing Flag-CaSR between *Kpn*I and *XbaI* (described previously[35]) was digested with *Bam*HI and *XbaI*, and the $GABA_{B2}$(760−941) PCR product was ligated with the digested vector to generate Flag-CaSR(908)-$GABA_{B2}$(760−941). Phe801^{ICL3}Ala and Glu837$^{7.32}$Ile mutations were introduced into the Flag-CaSR(908)-$GABA_{B2}$(760−941) using Quikchange mutagenesis (Agilent) (Phe801^{ICL3}Ala primers 5′cggaagctgccggagaacgccaatgaagccaagttcat and 3′atgaacttggcttcattggcgttctccggcagcttccg; Glu837$^{7.32}$Ile primers 5′gcaagtttgtctctgccgtaatagtgattgccatcctggcag and 3′ctgccaggatggcaatcactattacggcagagacaaacttgc). The latter construct is herein referred to as Flag-CaSR(F801A E837I 908)$_{B2}$.

Cell Culture. FlpIn HEK293 cells were maintained in DMEM with 5% FBS. FlpIn TRex HEK293 cells stably expressing the cmyc-tagged WT and mutant CaSRs have been described previously.[4,14] FlpIn TRex HEK293 WT and mutant CaSR cells were maintained in DMEM supplemented with 5% FBS, 200 μg/mL hygromycin, and 5 μg/mL blasticidin. For the generation of FlpIn HEK293 cells stably expressing a CaSR lacking its N-terminal VFT domain, cells were transfected with an N terminally truncated CaSR[36] modified for enhanced cell surface expression and detection (N terminal insertion of the influenza hemagglutinin signal peptide sequence followed by a double cmyc tag).[4] Cells transfected with the N terminally truncated CaSR were selected in DMEM containing 5% FBS and 400 μg/mL G418, and sorted into a 96 well plate into single cell populations using a MoFlo Astrios fluorescence activated cell sorter (FACS) (Beckman Coulter). Single cell populations were grown in selection media and analyzed for expression using flow cytometry with a FACS Canto (Beckman Coulter) as described previously.[4] The clonal population of cells exhibiting the highest N terminally truncated CaSR cell surface expression level was used for subsequent experiments.

Transient Transfection of cmyc-CaSR(908)$_{B1}$ and Flag-CaSR(F801A E837I 908)$_{B2}$. FlpIn HEK293 cells were seeded into T75 cm^2 flasks and transfected when they reached ∼80% confluence. On the day of transfection, growth media (DMEM with 5% FBS) was replaced. For each transfection, cells were transfected with a total of 20 μg of DNA consisting of (i) 10 μg of WT cmyc-CaSR (in pcDNA/frt/TO) plus 10 μg of pcDNA3.1+; (ii) 10 μg of WT Flag-CaSR (in pcDNA3.1+) plus 10 μg of pcDNA3.1+; (iii) 10 μg of cmyc-CaSR(908)$_{B1}$ (in pcDNA3.1+) plus 10 μg of pcDNA3.1+; (iv) 10 μg of Flag-CaSR(F801A E837I 908)$_{B2}$ (in pcDNA3.1+) plus 10 μg of pcDNA3.1+; (v) 10 μg of cmyc-CaSR(908)$_{B1}$ plus 10 μg of Flag-CaSR(F801A E837I 908)$_{B2}$; or (vi) 20 μg of pcDNA3.1+. DNA was diluted in 250 μL of NaCl, and mixed with 100 μg of PEI diluted in 250 μL of NaCl, for a 1:5 DNA:PEI ratio. The DNA:PEI mix was incubated for 10 min prior to addition to flasks. Cells were incubated for 24 h, after which they were harvested with 2 mM EDTA in PBS, centrifuged (350*g*, 10 min), and resuspended in 10 mL growth media. Cells were counted and plated into 96 well plates at 40 000 cells/well and incubated for a further 24 h, after which receptor cell surface expression and signaling were analyzed using flow cytometry analysis and Ca^{2+}i mobilization assays (described below).

Flow Cytometry Analysis for Receptor Expression. For expression measurements of cmyc-CaSR WT, Flag-CaSR WT, cmyc-CaSR(908)$_{B1}$, and Flag-CaSR(F801A E837I 908)$_{B2}$, transient transfections and cell plating is described above. For expression measurements of cmyc-CaSR following overnight treatment of CaSR-HEK293 cells with allosteric modulators, cells were seeded in a 96-well plate at a density of 80,000 cells/well in DMEM containing 100 ng mL-1 tetracycline and 3 μM allosteric modulator and incubated overnight at 37 °C.

On the day of the flow cytometry experiment, cells were harvested with PBS supplemented with 0.1% BSA, 2 mM EDTA and 0.05% NaN_3 (washing buffer) and transferred to wells of a 96 well v-bottom plate, centrifuged for 3 min at 350 x *g*, 4 °C and resuspended in 50−100 μL blocking buffer (PBS,

DOI: 10.1021/acsptsci.8b00021
ACS Pharmacol. Transl. Sci. 2018, 1, 96−109

5% BSA, 2 mM EDTA and 0.05% NaN_3) containing 1 μg/mL AF647-conjugated 9E10 antibody or FITC-conjugated anti-Flag antibody. Cells were incubated for 30−60 min at 4 °C and were subsequently washed with washing buffer and resuspended in washing buffer containing a dead cell stain (Sytox blue or propidium iodide). Receptor cell surface expression was quantified using a FACS Canto (Becton Dickinson) via detection of fluorescent antibodies bound to live cells.

IP1 Accumulation Assays. Cells grown in a T175 cm^2 flask were treated overnight with 100 ng/mL tetracycline. The following day, cells were harvested with 2 mM EDTA in PBS, and resuspended in assay buffer (150 mM NaCl, 2.6 mM KCl, 1.18 mM $MgCl_2$, 10 mM D-glucose, 10 mM HEPES, 0.1 mM or 1.2 mM $CaCl_2$, 50 mM LiCl, pH 7.4). Agonist, vehicle or modulator, were added to wells of a 384-well white proxiplate (PerkinElmer), followed by 10 000 cells, and plates were centrifuged for 1 min at 350*g* and incubated at 37 °C for 45 min. In some experiments, cells were preincubated with the PKC inhibitor, Go 6983 (1 μM), for 30 min before being added to wells containing ligands. IP1 accumulation was determined using an IP-One Tb assay kit (CisBio Bioassays, Codolet, France) according to manufacturer's instructions, with the exception that d2-conjugated IP1 and Lum4-Tb cryptate conjugated anti-IP1 antibody were diluted 1:35. FRET between labeled IP1 and anti-IP1 antibody was detected using an Envision plate reader (PerkinElmer). Results were calculated from the ratio of Lumi4-Tb cryptate conjugated anti-IP1 antibody emission at 620 nm over d2-conjugated IP1 emission at 665 nm. Data were normalized to the maximum response stimulated by $Ca^{2+}{}_o$ in the absence of modulator.

PTH Release Studies. Normal human parathyroid cells were obtained by collagenase-digestion after neck surgery[37] (procedures performed under institutional ethical guidelines and with patients' written informed consent). Stimulation of intact human PTH release from parathyroid cells perifused with buffer (125 mM NaCl, 4 mM KCl, 1.2 mM $CaCl_2$, 1 mM $MgCl_2$, 0.8 mM Na_2HPO_4, 20 mM HEPES, 0.1% D-glucose, 2.8 mM basal amino acid mixture, 1 mg/mL BSA, pH 7.4), was performed in the presence of increasing modulator concentrations. Intact human PTH was quantified by a two-site chemiluminescence ELISA on an Immulite 2000 autoanalyser as described previously.[37,38]

$Ca^{2+}{}_i$ Mobilization Assays. FlpIn HEK293 TRex stable cell lines were seeded at a density of 80 000 cells/well in clear 96-well plates coated with poly D-lysine (50 μg/mL) and incubated overnight in the presence of 100 ng/mL tetracycline. Transiently transfected FlpIn HEK293 cells were seeded at a density of 40 000 cells/well. The following day, cells were washed with assay buffer (150 mM NaCl, 2.6 mM KCl, 1.18 mM $MgCl_2$, 10 mM D-glucose, 10 mM HEPES, 0.1 or 1.2 mM $CaCl_2$, 0.5% BSA, 4 mM probenecid, pH 7.4) and loaded with 1 μM Fluo-4 AM in assay buffer. After 1 h at 37 °C, Fluo-4 AM was removed prior to the addition of fresh assay buffer. In functional interaction studies between CaSR agonists and modulators, modulators were either coadded with the agonist (coaddition paradigm), or preincubated for 20 min prior to the addition of agonist (preincubation paradigm).

The peak $Ca^{2+}{}_i$ mobilization response to agonists was measured at 37 °C, unless otherwise indicated, on a Flexstation 1 or 3 (Molecular Devices; Sunnyvale, CA, USA) using 485 nm excitation and 525 nm emission. Data were normalized to the maximum response produced by 1 μM ionomycin to account for differences in cell number and Fluo-4 AM loading efficiency.

Data Analysis. GraphPad Prism 6 or 7 (GraphPad Software, San Diego, CA, USA) was used for nonlinear regression analysis. Parametric measures of potency, affinity, and cooperativity were estimated as logarithms.

Concentration−response data at WT, 7TM domain mutant CaSRs, cmyc-CaSR(908)$_{B1}$, and Flag-CaSR(F801A E837I 908)$_{B2}$ were fitted to the following four-parameter concentration−response curve equation:

$$\text{response} = \frac{\text{basal} + (E_{max} - \text{basal}) \times [A]^{nH}}{[A]^{nH} + EC_{50}{}^{nH}} \quad (1)$$

where "response" is the response to the agonist, *n*H is the Hill slope, and basal and E_{max} represent the bottom and top asymptotes of the curve, respectively. EC_{50} is the concentration of agonist [A] that gives the midpoint response between basal and maximal effect.

Concentration−response data at an N terminally truncated CaSR were fitted as logarithms to the following biphasic concentration−response curve equation:

$$\text{response} = \text{fraction 1}\left(\frac{\text{basal} + (E_{max\_1} - \text{basal}) \times [A]^{nH\_1}}{[A]^{nH\_1} + EC_{50\_1}{}^{nH\_1}}\right) + \left(\frac{(E_{max\_2}) \times [A]^{nH\_2}}{[A]^{nH\_2} + EC_{50\_2}{}^{nH\_2}}\right) \quad (2)$$

where fraction 1 is the proportion of the total response due to the more potent response phase, E_{max_1} and E_{max_2} are the maximal agonist response for phase 1 and 2, respectively, EC_{50_1} and EC_{50_2} are the concentrations of agonist [A] that give the half maximal effect for phase 1 and 2, respectively, and *n*H_1 and *n*H_2 are the Hill slopes for phases 1 and 2, respectively.

Where calhex231 was a pure NAM (e.g., AC265347 versus calhex231 interactions), data were fitted to the following operational model of allosterism:

$$\text{response} = (E_{max}(\tau_A[A + C](K_B + \alpha\beta[B]) + \tau_B[B][K_A])^n) / (([A + C]K_B + K_AK_B + K_A[B] + \alpha[A + C][B])^n + (\tau_A[A](K_B + \alpha\beta[B]) + \tau_B[B]K_A)^n) \quad (3)$$

where [A+C] denotes the total orthosteric agonist concentration including the ambient (contaminating) agonist; [B] denotes the allosteric ligand concentration; K_A and K_B are the functional affinities of orthosteric and allosteric ligands, respectively; τ_A and τ_B represent the efficacy of orthosteric and allosteric ligands respectively; α and β denote allosteric effects on orthosteric ligand binding affinity and efficacy, respectively; *n* is the transducer slope.

Where calhex231 was a pure PAM (e.g., $Ca^{2+}{}_o$ versus calhex231 at the Phe688$^{3.40}$Ala mutant CaSR and at the cmyc-CaSR(908)$_{B1}$/Flag-CaSR(F801A E837I 908)$_{B2}$ heterodimer, functional interaction studies were fitted to the following operational model of allosterism:

$$\text{response} = \frac{(E_{max} - \text{basal})([A + C](K_B + \alpha\beta[B]) + \tau_B[B][EC_{50}])}{EC_{50}(K_B + [B]) + ([A + C](K_B + \alpha\beta[B]) + \tau_B[B]EC_{50}])} \quad (4)$$

where the parameters are as described for equations 1 and (3).

DOI: 10.1021/acsptsci.8b00021
ACS Pharmacol. Transl. Sci. 2018, 1, 96−109

Data Simulations. The effects of an allosteric modulator that binds to two allosteric sites on agonist binding were simulated using the following allosteric quaternary complex model:

$$\text{agonist binding} = \frac{B_{max} \times \frac{[A+C]}{B_{mid}}}{1 + \frac{[A+C]}{B_{mid}}}$$

where

$$B_{mid} = K_A\left[\frac{1 + ([B]/K_B) + ([B]/K_C)[1 + \delta([B]/K_B)]}{1 + \alpha([B]/K_B) + \beta([B]/K_C)[1 + \alpha\gamma]([B]/K_B)}\right] \quad (5)$$

[A+C] is the orthosteric agonist concentration including the ambient (contaminating) agonist; [B] is the allosteric ligand concentration; K_A is the equilibrium dissociation constant of the orthosteric ligand; K_B is the equilibrium dissociation constant of the allosteric ligand for site 1; K_C is the equilibrium dissociation constant of the allosteric ligand for site 2; α is the cooperativity between the orthosteric agonist and modulator bound to site 1; β is the cooperativity between the orthosteric agonist and modulator bound to site 2; (vi) δ is the cooperativity between the allosteric modulator and itself (i.e., between sites 1 and site 2) when the orthosteric agonist is absent; and (vii) γ is the cooperativity between the allosteric modulator and itself when the orthosteric agonist occupies the receptor.

Statistics. Statistical differences between the $Ca^{2+}{}_o$ E_{max} or pEC_{50} in the absence or presence of modulator were determined by an extra sum-of-squares F test, followed by a one-way ANOVA with Dunnett's multiple comparisons post-test. A one-way ANOVA with Dunnett's multiple comparisons post-test was used to determine statistical differences between the calhex231 pK_B and $\log \alpha\beta$ at the WT versus the mutant receptors. A two-way repeated measures ANOVA with Dunnett's multiple comparisons post-test was used to determine statistical differences between basal PTH levels and those following primary parathyroid cell exposure to modulators at different time points post-modulator exposure. Statistical differences between the N terminally truncated CaSR response to 2 and 14 mM $Ca^{2+}{}_o$ in the absence or presence of calhex231 were determined by student's t test. $p < 0.05$ was considered statistically significant.

Molecular Modeling and Docking Studies. A three-dimensional model of the CaSR 7TM domain was constructed by homology with $mGlu_5$ (PDB: 5CGD)[20] using the ICM software package[39] (Molsoft; San Diego, USA) as previously described.[4] The 7TM helices in the model were additionally refined to accommodate irregularities such as nonconserved proline residues (e.g., $Pro682^{3.34}$) and a one-residue insertion in the extracellular part of TM5 ($Ile777^{5.44}$). Compound docking relied on the pharmacophore properties of the TM cavity as well as the results of earlier and present mutagenesis studies indicating that mutation of $Glu837^{7.32}$ abrogates activity of all arylalkylamines. This is predicted to be due to a critical salt bridge between the protonated arylalkylamine secondary amine and the $Glu837^{7.32}$ side chain;[4,6−8,40] therefore, the formation of this salt bridge was enforced in our docking studies by imposing a harmonic distance restraint between the corresponding atoms. The arylalkylamine docking proceeded by extensive conformational sampling of the ligands and the residue side chains lining the pocket in internal coordinates in the presence of this distance restraint. All complexes were further refined by local minimization in the presence of distance restraints maintaining receptor secondary and tertiary structures, and inspected manually.

■ ASSOCIATED CONTENT

Supporting Information

The Supporting Information is available free of charge on the ACS Publications website at DOI: 10.1021/acsptsci.8b00021.

Additional figures and tables as described in the text (PDF)

■ AUTHOR INFORMATION

Corresponding Author

*Tel.: +61 3 99039089. E-mail: katie.leach@monash.edu.

ORCID

Ben Capuano: 0000-0001-5434-0180

Katie Leach: 0000-0002-9280-1803

Author Contributions

K.L., K.J.G., A.D.C., and A.C. contributed to study design and provided overall project supervision; K.L., K.J.G., A.N.K., and E.K. performed HEK293 cell expression, signaling, and mutagenesis assays; H.M. performed PTH release assays; M.A.G. and A.N.K. generated cmyc-$CaSR(908)_{B1}$ and Flag-$CaSR(F801A\ E837I\ 908)_{B2}$ constructs; K.L. and K.J.G. performed data analysis and simulations; I.K. performed molecular modeling and modulator docking studies; K.L., K.J.G., I.K., A.N.K., E.K., R.M., B.C., A.D.C., and A.C. contributed to writing the manuscript.

Notes

The authors declare no competing financial interest.

■ ACKNOWLEDGMENTS

Thanks go to Alisha Panwar and Aaron P Townley for their contribution to experiments in HEK293 cells. This work was supported by National Health and Medical Research Council of Australia (NHMRC) Project Grant APP1085143, and by and the National Institutes of Health National Institute of General Medical Sciences and National Institute of Allergy and Infectious Diseases Grants GM117424 and AI118985, respectively. K.L. and K.J.G. are Australian Research Council Future Fellows. A.C. is a Senior Principal Research Fellow of the NHMRC.

■ REFERENCES

(1) Brown, E. M. (2013) Role of the calcium-sensing receptor in extracellular calcium homeostasis. *Best Pract Res. Clin Endocrinol Metab 27*, 333−43.

(2) Leach, K., Sexton, P. M., Christopoulos, A., and Conigrave, A. D. (2014) Engendering biased signalling from the calcium-sensing receptor for the pharmacotherapy of diverse disorders. *Br. J. Pharmacol. 171*, 1142−55.

(3) Leach, K., and Gregory, K. J. (2017) Molecular insights into allosteric modulation of Class C G protein-coupled receptors. *Pharmacol. Res. 116*, 105−118.

(4) Leach, K., et al. (2016) Towards a structural understanding of allosteric drugs at the human calcium sensing receptor. *Cell Res. 26*, 574−92.

(5) Keller, A. N., et al. (2018) Identification of Global and Ligand-Specific Calcium Sensing Receptor Activation Mechanisms. *Mol. Pharmacol. 93*, 619−630.

(6) Miedlich, S. U., Gama, L., Seuwen, K., Wolf, R. M., and Breitwieser, G. E. (2004) Homology modeling of the transmembrane

DOI: 10.1021/acsptsci.8b00021
ACS Pharmacol. Transl. Sci. 2018, 1, 96−109

domain of the human calcium sensing receptor and localization of an allosteric binding site. *J. Biol. Chem. 279*, 7254−63.
(7) Petrel, C., et al. (2004) Positive and negative allosteric modulators of the Ca2+-sensing receptor interact within overlapping but not identical binding sites in the transmembrane domain. *J. Biol. Chem. 279*, 18990−7.
(8) Petrel, C., et al. (2003) Modeling and mutagenesis of the binding site of Calhex 231, a novel negative allosteric modulator of the extracellular Ca(2+)-sensing receptor. *J. Biol. Chem. 278*, 49487−94.
(9) Dore, A. S., et al. (2014) Structure of class C GPCR metabotropic glutamate receptor 5 transmembrane domain. *Nature 511*, 557−62.
(10) Kessler, A., et al. (2006) N1-Benzoyl-N2-[1-(1-naphthyl)-ethyl]-trans-1,2-diaminocyclohexanes: Development of 4-chlorophenylcarboxamide (calhex 231) as a new calcium sensing receptor ligand demonstrating potent calcilytic activity. *J. Med. Chem. 49*, 5119−28.
(11) Gregory, K. J., et al. (2012) Investigating metabotropic glutamate receptor 5 allosteric modulator cooperativity, affinity, and agonism: enriching structure-function studies and structure-activity relationships. *Mol. Pharmacol. 82*, 860−75.
(12) Sengmany, K., et al. (2017) Biased allosteric agonism and modulation of metabotropic glutamate receptor 5: Implications for optimizing preclinical neuroscience drug discovery. *Neuropharmacology 115*, 60−72.
(13) Nickols, H. H., et al. (2016) VU0477573: Partial Negative Allosteric Modulator of the Subtype 5 Metabotropic Glutamate Receptor with In Vivo Efficacy. *J. Pharmacol. Exp. Ther. 356*, 123−36.
(14) Davey, A. E., et al. (2012) Positive and negative allosteric modulators promote biased signaling at the calcium-sensing receptor. *Endocrinology 153*, 1232−41.
(15) Cook, A. E., et al. (2015) Biased allosteric modulation at the CaSR engendered by structurally diverse calcimimetics. *Br. J. Pharmacol. 172*, 185−200.
(16) Lorenz, S., Frenzel, R., Paschke, R., Breitwieser, G. E., and Miedlich, S. U. (2007) Functional desensitization of the extracellular calcium-sensing receptor is regulated via distinct mechanisms: role of G protein-coupled receptor kinases, protein kinase C and beta-arrestins. *Endocrinology 148*, 2398−404.
(17) Grant, M. P., Stepanchick, A., Cavanaugh, A., and Breitwieser, G. E. (2011) Agonist-driven maturation and plasma membrane insertion of calcium-sensing receptors dynamically control signal amplitude. *Sci. Signaling 4*, ra78.
(18) Diepenhorst, N. A., Leach, K., Keller, A. N., Rueda, P., Cook, A. E., Pierce, T. L., Nowell, C., Pastoureau, P., Sabatini, M., and Langmead, C. J. et al. (2018)Divergent effects of strontium and calcium-sensing receptor positive allosteric modulators (calcimimetics) on human osteoclast activity, *Br. J. Pharmacol.*. DOI: 10.1111/bph.14344
(19) Geng, Y., Mosyak, L., Kurinov, I., Zuo, H., Sturchler, E., Cheng, T. C., Subramanyam, P., Brown, A. P., Brennan, S. C., Fan, Q. R., et al. (2016) Structural mechanism of ligand activation in human calcium-sensing receptor. *eLife 5*, No. e13662, DOI: 10.7554/eLife.13662.
(20) Christopher, J. A., et al. (2015) Fragment and Structure-Based Drug Discovery for a Class C GPCR: Discovery of the mGlu5 Negative Allosteric Modulator HTL14242 (3-Chloro-5-[6-(5-fluoropyridin-2-yl)pyrimidin-4-yl]benzonitrile). *J. Med. Chem. 58*, 6653−64.
(21) Nemeth, E. F., et al. (2004) Pharmacodynamics of the type II calcimimetic compound cinacalcet HCl. *J. Pharmacol. Exp. Ther. 308*, 627−35.
(22) Kessler, A., et al. (2004) N2-benzyl-N1-(1-(1-naphthyl)ethyl)-3-phenylpropane-1,2-diamines and conformationally restrained indole analogues: development of calindol as a new calcimimetic acting at the calcium sensing receptor. *Bioorg. Med. Chem. Lett. 14*, 3345−9.
(23) Gowen, M., et al. (2000) Antagonizing the parathyroid calcium receptor stimulates parathyroid hormone secretion and bone formation in osteopenic rats. *J. Clin. Invest. 105*, 1595−604.
(24) Balan, G., et al. (2009) The discovery of novel calcium sensing receptor negative allosteric modulators. *Bioorg. Med. Chem. Lett. 19*, 3328−32.
(25) Tomé, L. I. N., Rosado, M. T. S., Eusébio, M. E. S., and Redinha, J. S. (2007) Molecular structure of mono- and 1,2-aminoderivatives of cyclohexane: Steric strain effects as determining factors. *J. Mol. Struct.: THEOCHEM 804*, 65−74.
(26) Kay, J. B., Robinson, J. B., Cox, B., and Polkonjak, D. (1970) 1,2-disubstituted cyclohexanes as substrates of acetylcholinesterase and muscarinic agents. A re-investigation. *J. Pharm. Pharmacol. 22*, 214−21.
(27) Jacobsen, S. E., Gether, U., and Brauner-Osborne, H. (2017) Investigating the molecular mechanism of positive and negative allosteric modulators in the calcium-sensing receptor dimer. *Sci. Rep. 7*, 46355.
(28) El Moustaine, D., et al. (2012) Distinct roles of metabotropic glutamate receptor dimerization in agonist activation and G-protein coupling. *Proc. Natl. Acad. Sci. U. S. A. 109*, 16342−7.
(29) Kammerer, R. A., et al. (1999) Heterodimerization of a functional GABAB receptor is mediated by parallel coiled-coil alpha-helices. *Biochemistry 38*, 13263−9.
(30) Margeta-Mitrovic, M., Jan, Y. N., and Jan, L. Y. (2000) A trafficking checkpoint controls GABA(B) receptor heterodimerization. *Neuron 27*, 97−106.
(31) Pagano, A., et al. (2001) C-terminal interaction is essential for surface trafficking but not for heteromeric assembly of GABA(b) receptors. *J. Neurosci. 21*, 1189−202.
(32) Lanzafame, A. A., Sexton, P. M., and Christopoulos, A. (2006) Interaction studies of multiple binding sites on m4 muscarinic acetylcholine receptors. *Mol. Pharmacol. 70*, 736−46.
(33) Goudet, C., et al. (2005) Asymmetric functioning of dimeric metabotropic glutamate receptors disclosed by positive allosteric modulators. *J. Biol. Chem. 280*, 24380−5.
(34) Hlavackova, V., et al. (2005) Evidence for a single heptahelical domain being turned on upon activation of a dimeric GPCR. *EMBO J. 24*, 499−509.
(35) Bai, M., et al. (1996) Expression and characterization of inactivating and activating mutations in the human Ca2+o-sensing receptor. *J. Biol. Chem. 271*, 19537−45.
(36) Mun, H. C., et al. (2004) The Venus Fly Trap domain of the extracellular Ca2+ -sensing receptor is required for L-amino acid sensing. *J. Biol. Chem. 279*, 51739−44.
(37) McCormick, W. D., et al. (2010) Increased receptor stimulation elicits differential calcium-sensing receptor(T888) dephosphorylation. *J. Biol. Chem. 285*, 14170−7.
(38) Mun, H. C., et al. (2009) Adenomatous human parathyroid cells exhibit impaired sensitivity to L-amino acids. *J. Clin. Endocrinol. Metab. 94*, 3567−74.
(39) Abagyan, R., and Totrov, M. (1994) Biased probability Monte Carlo conformational searches and electrostatic calculations for peptides and proteins. *J. Mol. Biol. 235*, 983−1002.
(40) Bu, L., Michino, M., Wolf, R. M., and Brooks, C. L. (2008) Improved model building and assessment of the Calcium-sensing receptor transmembrane domain. *Proteins: Struct., Funct., Genet. 71*, 215−26.

DOI: 10.1021/acsptsci.8b00021
ACS Pharmacol. Transl. Sci. 2018, 1, 96−109